Recognition of DNA adducts by edited and unedited forms of DNA glycosylase NEIL1

Irina G. Minko[a], **Vladimir L. Vartanian**[a], **Naoto N. Tozaki**[a], **Erdem Coskun**[b,c], **Sanem Hosbas Coskun**[b], **Pawel Jaruga**[b], **Jongchan Yeo**[d], **Sheila S. David**[d], **Michael P. Stone**[e], **Martin Egli**[f], **Miral Dizdaroglu**[b], **Amanda K. McCullough**[a,g], **R. Stephen Lloyd**[a,g,h,*]

[a]Oregon Institute of Occupational Health Sciences, Oregon Health & Science University, Portland, OR 97239, United States

[b]Biomolecular Measurement Division, National Institute of Standards and Technology, Gaithersburg, MD 20899, United States

[c]Institute for Bioscience and Biotechnology Research, University of Maryland, Rockville, MD 20850, United States

[d]Department of Chemistry, University of California, Davis, CA, 95616, United States

[e]Department of Chemistry, Vanderbilt University, Nashville, TN, 37235, United States

[f]Department of Biochemistry, Vanderbilt University, Nashville, TN, 37232, United States

[g]Department of Molecular and Medical Genetics, Oregon Health & Science University, Portland, OR 97239, United States

[h]Department of Physiology and Pharmacology, Oregon Health & Science University, Portland, OR 97239, United States

Abstract

Pre-mRNA encoding human NEIL1 undergoes editing by adenosine deaminase ADAR1 that converts a single adenosine to inosine, and this conversion results in an amino acid change of lysine 242 to arginine. Previous investigations of the catalytic efficiencies of the two forms of the enzyme revealed differential release of thymine glycol (ThyGly) from synthetic oligodeoxynucleotides, with the unedited form, NEIL1 K242 being ≈30-fold more efficient than the edited NEIL1 K242R. In contrast, when these enzymes were reacted with oligodeoxynucleotides containing guanidinohydantoin or spiroiminohydantoin, the edited K242R form was ≈3-fold more efficient than the unedited NEIL1. However, no prior studies have investigated the efficiencies of these two forms of NEIL1 on either high-molecular weight DNA containing multiple oxidatively-induced base damages, or oligodeoxynucleotides containing a bulky alkylated formamidopyrimidine. To understand the extent of changes in substrate recognition, γ-irradiated calf thymus DNA was treated with either edited or unedited NEIL1 and the released DNA base lesions analyzed by gas chromatography-tandem mass spectrometry. Of all

*To whom correspondence should be sent: Tel: 503-494-9957; Fax: 503-494-6831; lloydst@ohsu.edu.

the measured DNA lesions, imidazole ring-opened 4,6-diamino-5-formamidopyrimidine (FapyAde) and 2,6-diamino-4-hydroxy-5-formamidopyrimidine (FapyGua) were preferentially released by both NEIL1 enzymes with K242R being $\approx$1.3 and 1.2-fold more efficient than K242 on excision of FapyAde and FapyGua, respectively. Consistent with the prior literature, large differences ($\approx$7.5 to 12-fold) were measured in the excision of ThyGly from genomic DNA by the unedited versus edited NEIL1. In contrast, the edited NEIL1 was more efficient ($\approx$3 to 5-fold) on release of 5-hydroxy-cytosine. Excision kinetics on DNA containing a site-specific aflatoxin B_1-FapyGua adduct revealed an $\approx$1.4-fold higher rate by the unedited NEIL1. Molecular modeling provides insight into these differential substrate specificities. The results of this study and in particular, the comparison of substrate specificities of unedited and edited NEIL1 using biologically and clinically important base lesions, are critical for defining its role in preservation of genomic integrity.

Keywords

base excision repair; RNA editing; formamidopyrimidines; thymine glycol; aflatoxin; hepatocellular carcinoma

1. Introduction

The fundamental steps defining the DNA base excision repair (BER) pathway are conserved across all organisms, with altered or damaged bases being detected and removed by DNA glycosylases. Not surprisingly, due to the intrinsic properties of DNA that render it susceptible to base changes such as exocyclic deamination, ring saturation, ring fragmentation, oxidation, and alkylation, DNA glycosylases generally possess broad substrate specificities to confer genomic stability through limiting mutagenesis that can occur from error-prone translesion synthesis past these lesions (reviewed in (1, 2)). Factors that modulate the activities of these enzymes include, but are not limited to, tissue-specific expression, stages in the cell cycle when damage is either produced or detected, post-translational modifications, gene expression profiles, chromatin structure, and RNA editing (reviewed in (3-7)).

Reactive oxygen species that are generated via ionizing radiation, heavy metals, and numerous physiological pathways constitute one of the most common sources of DNA base damage. These exposures can generate imidazole ring-fragmented purines, saturated pyrimidines, and oxidized adenines or guanines, including 8-hydroxyguanine (8-OH-Gua) (reviewed in (1)). In mammalian cells, a series of DNA glycosylases recognize and initiate repair of these lesions, including NEIL1, NEIL2, NEIL3, OGG1, and NTH1 (reviewed in (1)). The discovery and characterization of the *NEIL* genes were initially reported by multiple laboratories (8-10). Using site-specifically modified oligodeoxynucleotides and irradiated genomic DNAs, the NEIL1 substrates included 4,6-diamino-5-formamidopyrimidine (FapyAde), 2,6-diamino-4-hydroxy-5-formamidopyrimidine (FapyGua) (9, 11), thymine glycol (ThyGly) and a subset of saturated and deaminated pyrimidines (8-12). Although the excision of 8-OH-Gua by human NEIL1 has been reported (10), many other *in vitro* and *in vivo* studies have not confirmed this activity (reviewed in

(1)). However, the secondary oxidation products of 8-OH-Gua, guanidinohydantoin (Gh) and its isomer, iminoallantoin, both diastereomers of spiroiminodihydantoin (Sp1 and Sp2), and two diastereomers of 5-carboxamido-5-formamido-2-iminohydantoin (R)-2Ih and (S)-2Ih have been found to be excellent substrates for NEIL1 (13-18). Additional base damage substrates for NEIL1 that have been identified using synthetic oligodeoxynucleotide substrates include: psoralen-induced DNA crosslinks in 3-stranded structures (19), psoralen-induced 4-stranded crosslinks (20), 5-carboxylcytosine (21), methyl-FapyGua (16), amine adducts of hydantoins (22), 8,9-dihydro-8-(2,6-diamino-4-oxo-3,4-dihydropyrimid-5-yl-formamido)-9-hydroxyaflatoxin B_1 (AFB$_1$-FapyGua)(23, 24), and nitrogen mustard-FapyGua (25).

It has previously been demonstrated that the pre-mRNA encoding NEIL1 undergoes editing by adenosine deaminase, ADAR1, with deamination of C6 at adenosine 726 to form inosine (26, 27). Since inosine codes as guanosine during translation, this edited mRNA changes the amino acid codon at position 242 from lysine (K) to arginine (R). Although the biological significance of the K242R change has not been well elucidated, ADAR1 expression is induced by a variety of stressors, including interferon α (26, 28). This may explain an aberrant hyper-editing of NEIL1 that was found in multiple myeloma cell lines and patient samples (29). Analyses of cell lines with low ADAR1 levels and expressing K242 and K242R suggested functional differences of these NEIL1 forms, with the edited form conferring higher growth rates, enhanced cell cycles progression, and upregulation of markers of DNA double-strand breaks (29).

The vast majority of prior studies on the substrate specificity of NEIL1 have used the edited form. However, comparative analyses of K242 versus K242R revealed that the catalytic efficiency of these enzymes on oligodeoxynucleotides containing site specific lesions could vary greatly. Specifically, the K242 removed ThyGly ≈ 30-fold more efficiently than K242R, while the edited form was more efficient on oligodeoxynucleotides containing Gh and Sp lesions (26). The increased efficiency of incision by the K242 on ThyGly-containing substrates has been confirmed (16, 30). To further understand the basis for these differences, binding studies were carried out with the two NEIL1 forms with oligodeoxynucleotides containing 2′-fluorothymidine glycol in either a ribo- or arabino-configuration (31). Since binding affinities were similar for both K242 and K242R, these data suggested that the effects of editing on substrate specificity are related to a kinetic base excision step rather than ThyGly recognition.

Given that current data on the substrate specificity of the unedited NEIL1 have been limited and that all previous characterizations of this enzyme have been carried out using synthetic oligodeoxynucleotides, the purpose of this investigation was to expand the understanding of the substrate differences between the two forms of NEIL1 using damaged genomic DNA with multiple lesions. In addition, considering the protective role of NEIL1 in formation of aflatoxin B_1 (AFB$_1$)-induced hepatocellular carcinoma (HCC) in mice (23), the two forms of NEIL1 were compared on oligodeoxynucleotides containing the AFB$_1$-FapyGua adduct.

2. Materials and Methods

2.1. Expression constructs

Procedures for the construction of the pET22b(+) vector for expression of the edited human NEIL1 were previously described (26, 32). The corresponding vector for expression of the unedited NEIL1 was created using Q5 Site-Directed Mutagenesis Kit (New England BioLabs). Following plasmid isolation, the expected substitution was confirmed by Sanger sequencing and the sequence of the open reading frame coding for the unedited NEIL1 with the C-terminal 6-His-tag was verified (DNA Sequencing Core, Vollum Institute, Oregon Health & Science University).

2.2. Expression and purification of NEIL1 enzymes

Expression and purification of NEIL1 enzymes were performed according to protocols initially developed for the edited NEIL1 (26, 32). The current version of these protocols was recently published (24).

2.3. Preparation of high-molecular DNA substrate for glycosylase reactions

Preparation of high-molecular DNA substrate from commercially available calf thymus DNA using a ^{60}Co γ-ray source was recently reported (24). DNA samples were γ-irradiated at a dose of either 5 Gy or 20 Gy.

2.4. NEIL1-catalyzed reactions using high-molecular weight DNA substrates and detection of excised DNA base lesions by gas chromatography-tandem mass spectrometry (GC-MS/MS)

For NEIL1-catalyzed reactions, aliquots of γ-irradiated DNA were supplemented with aliquots of stable isotope-labeled analogues of DNA base lesions as internal standards. Incubation of DNA samples with unedited and edited NEIL1, with subsequent analysis of the released DNA base lesions by gas chromatography-tandem mass spectrometry (GC-MS/MS) was performed as described in our prior studies (24, 33). The measured levels of the excised DNA base lesions were expressed as number of lesions per 10^6 DNA bases. The mean values with standard deviations were calculated from the measurements of twelve independently prepared DNA samples, and analyzed using KaleidaGraph software (Synergy Software).

2.5. DNA glycosylase assays using oligodeoxynucleotides with a site-specific AFB$_1$-FapyGua

Procedures for synthesis of 24-mer oligodeoxynucleotide containing AFB$_1$-FapyGua (5′-ACCACTACTATXATTCATAACAAC-3′ where X denotes site of modification) were previously reported (34). The complementary oligodeoxynucleotide (5′-GTTGTTATGAATCATAGTAGTGGT-3′) that was designed to have a cytosine opposite the lesion was synthesized by Integrated DNA Technologies. The double-stranded DNA substrate, with the adducted strand labeled with ^{32}P at the 5′ terminus was prepared as described in our prior study (23).

The rate constants for NEIL1-catalyzed excision of AFB$_1$-FapyGua were measured under single turnover conditions as previously described (23, 24). DNA substrate and enzyme concentrations were 20 nmol/L and 500 nmol/L, respectively. The reactions were performed at 37 °C. DNA was separated by gel electrophoresis under denaturing conditions (polyacrylamide gel containing 8 mol/L urea and DNA samples containing 63 % (v/v) formamide). The reaction products were visualized using a Personal Molecular Imager System (Bio-Rad) and quantified from a phosphor screen image by Quantity One Software (Bio-Rad). The rate constant was obtained from the best fit of the data to a single exponential equation using KaleidaGraph software.

2.6. Modeling FapyGua in the NEIL1 active site

The crystallographic coordinates for C-terminally truncated (95-CTD) K242 and K242R NEIL1 bound to duplex DNA containing ThyGly (30) were retrieved from the Protein Data Bank (www.rcsb.org; PDB ID 5ITX and 5ITY, respectively). The FapyGua was modeled in the NEIL1 active site in the β-anomeric configuration using the program UCSF Chimera (35). However, we retained the sugar-phosphate backbone conformation of the deoxynucleotide extruded from the duplex seen in the crystal structure of the NEIL1:ThyGly DNA complex. Of the four possible rotameric conformations of the formamide group, we used the conformation that previously was identified by NMR spectroscopy of the acetyl-protected monomeric FapyGua as the major species (the *cis*-amide conformer that is stabilized by a hydrogen bond between the carbonyl oxygen of the formamide and the NH of the glycosidic bond) (36). According to analyses by the density functional theory, this conformer (Z2 in the referenced study) is expected to be dominant in single-stranded DNA and exist in equilibrium with two other conformers (*E* and *Z*1) in double-stranded DNA (37). The FapyGua residue was modeled both in the *syn* and *anti* conformations. The active site NEIL1 structures with FapyGua were energy minimized with Amber 14 (38).

3. Results

3.1. Excision of oxidatively-induced base lesions from high-molecular weight DNA

To compare specificities of the unedited and edited forms of NEIL1 for oxidatively-induced DNA lesions, high-molecular weight calf thymus DNA was used that had been irradiated with γ-rays in aqueous buffered solution saturated with N$_2$O. The advantages of this approach include the simultaneous availability of a wide variety of pyrimidine- and purine-derived lesions in DNA for glycosylase-catalyzed excisions in a single reaction, lack of predetermination with regard to sequence context surrounding the lesion site, and much lower adduct concentrations per DNA size than in oligodeoxynucleotides, typically containing one DNA base lesion per 15 to 30 DNA bases. Thus, this experimental system can be considered a simplified model for intracellular conditions.

Following incubation of NEIL1 enzymes with DNA that was exposed to 5 Gy irradiation dose, four types of modified bases were detected above background levels: FapyAde, FapyGua, ThyGly, and 5-OH-Cyt (Fig. 1A). The two forms of NEIL1 showed no difference in their abilities to excise FapyAde or FapyGua under these experimental conditions (Fig. 1B & C). The level of ThyGly excised by K242 (corrected for non-enzyme specific hydrolysis)

was ≈7.5-fold higher than that produced by K242R (Fig. 1D). This result was consistent with prior data demonstrating that the unedited NEIL1 removed ThyGly from oligodeoxynucleotides more efficiently than the edited NEIL1 (16, 26). In contrast, K242R released ≈5-fold more 5-OH-Cyt relative to K242 (Fig. 1E).

Considering the possibility that release of FapyAde and FapyGua by NEIL1 enzymes was limited by the availabilities of these adducts in DNA, the dose of DNA irradiation was increased to 20 Gy and glycosylase reactions were repeated (Fig. 1, F-I). As a result of the increased irradiation, the levels of FapyAde excised by K242 and K242R increased by ≈2.7 and ≈3.3-fold, respectively (compare Figs. 1B & 1F). Release of FapyGua also increased, with ≈1.5 and ≈1.7-fold higher levels produced by K242 and K242R, respectively (compare Figs. 1C & 1G). The effect of editing on excision of FapyAde and FapyGua was apparent under these conditions. Relative to the unedited NEIL1, K242R released FapyAde with ≈1.3-fold higher efficiency (Fig. 1F) and FapyGua with ≈1.2-fold higher efficiency (Fig. 1G).

The data obtained using DNA that was exposed to 20 Gy dose also confirmed the conclusions on differential recognition of ThyGly and 5-OH-Cyt by two forms of NEIL1. Specifically, the level of ThyGly excised by K242 was ≈12.3-fold higher than that excised in the presence of K242R (Fig. 1H). In fact, there was no statistically significant difference between release of ThyGly following incubation with K242R and non-enzyme specific hydrolysis. K242R released ≈3-fold more 5-OH-Cyt relative to K242, with no statistically significant difference found between incubation with K242 versus no enzyme control reaction (Fig. 1I).

Interestingly, the 4-fold increase in DNA irradiation dose that resulted in significantly elevated levels of released FapyAde and FapyGua in the presence of NEIL1 enzymes had no or negative effect on excision of ThyGly and 5-OH-Cyt. Also, no evidence was found for NEIL1-catalyzed release of 8-OH-Ade, 8-OH-Gua, 5-OH-Ura, 5-OH-5-MeHyd, or 5,6-diOH-Ura. These data demonstrated that of all the measured oxidatively-induced DNA base lesions, FapyAde and FapyGua were highly preferred substrates for both edited and unedited NEIL1, and with regard to its edited form, also confirmed the previously published data (reviewed in (1)).

3.2. Removal of AFB$_1$-FapyGua

Using the edited NEIL1, we previously have demonstrated that this enzyme can catalyze excision of AFB$_1$-FapyGua from a synthetic oligodeoxynucleotide (23). AFB$_1$-FapyGua (Fig. 2A) is a chemically stable product of metabolically processed AFB$_1$, a known human hepatocarcinogen. AFB$_1$-FapyGua accumulates in tissues of exposed animals (23, 39, 40), is highly mutagenic (41), and its miscoding properties correlate with a mutagenic signature that is attributed to aflatoxin exposure (42-44). We also demonstrated that *Neil1$^{-/-}$* mice accumulated more of AFB$_1$-FapyGua in liver DNA than *Neil1$^{+/+}$* mice and that in a murine model, deficiency in NEIL1 was a risk factor for aflatoxin-induced HCC (23). Collectively, these observations implicate AFB$_1$-FapyGua as a significant contributor to hepatocarcinogenesis associated with aflatoxin exposure and suggest a protective role for NEIL1 in this process.

To compare rates of removal of AFB_1-FapyGua by the edited and unedited forms of NEIL1, enzymes were reacted with radioactively-labeled site-specifically modified oligodeoxynucleotides under single turnover conditions. The data generated for the edited NEIL1 have been reported in our recent investigations on rare NEIL1 variants found in East Asian populations (24). Representative gel images and plot demonstrating the time-dependent conversion of substrate to product are shown on Fig. 2B, 2C, and 2D, respectively. The average observed excision rate constants (k_{obs}) with standard deviations were calculated for each enzyme from three independent experiments. For the edited NEIL1, the rate was (0.18 ± 0.01) min^{-1}, which was in a good agreement with the rate of (0.17 ± 0.03) min^{-1} measured in our prior study (23). The rate of excision by the unedited NEIL1 was (0.26 ± 0.03) min^{-1}, $\approx$1.4-fold higher. The difference was statistically significant, with the p value of 0.04.

3.3. Modeling the structure of FapyGua in the NEIL1 active site

The structural basis for the differential excision of ThyGly by K242 and K242R has previously been addressed by analyzing the crystal structures of NEIL1 enzymes bound to DNA that contained either a stable analog of an abasic site or ThyGly (30). The 242 residue was shown to be located within a flexible loop (residues 240-252) that is involved in damage recognition. In structures with ThyGly, the nucleotide is flipped out of the duplex and relative to the native NEIL1 structure, the 242 residue undergoes flipping, with the side chain pointing toward the N3 atom of the base (Fig. 3A). The authors reasoned that such close proximity of two proton donors would be unfavorable and proposed that ThyGly tautomerization from the C2=O keto form to the C2-OH enol form would make the N3 position a hydrogen bond acceptor. Based on this observation and computational simulation, a ribose-protonated pathway was proposed, with the formed C2-OH group playing an integral role in the catalysis. The first step in the proposed pathway is ribose ring-opening that is facilitated by a protonated E3 and accompanied by the nucleophilic attack of P2. The positively charged P2 would then be deprotonated with the assistance of the C2-OH group which transfers a proton from P2 to E6. One of the functions of K242/R242 in this pathway is protonation of the base, specifically at N3, which is a concluding step in scission of the glycosidic bond. Since the K242 would be a better electron donor than R242 based on a lower pK_a, the more efficient excision of ThyGly by the unedited NEIL1 is highly consistent with the proposed model. The critical nature of the basic residue at position 242 in base excision was reinforced by site-directed mutagenesis and kinetic assays in which K242A, K242E, and K242Q were all severely compromised in glycosylase, but not AP lyase activities (30).

However, these analyses have been conducted on a relatively poor substrate for NEIL1 and not on its dominant, purine-derived substrates. Thus, we modeled FapyGua into the crystal structure of K242 NEIL1 (P2G mutant, C-95) complexed with DNA containing ThyGly (PDB ID 5ITX) (30). The FapyGua residue was modeled both in the *anti* and *syn* conformations around the glycosidic bond (Fig. 3B and 3C, respectively). These analyses demonstrated that FapyGua could not be accommodated in the NEIL1 active site in the *anti* conformation (Fig. 3B). This conformation creates a clash between the hydrogen-bonding face of FapyGua and active site residues E6 and K242 (circled in Fig. 3B), suggesting that

either rearrangements of flexible loop occur which are accompanied by major structural changes in the NEIL1 active site or the modified base assumes an alternative conformation. Consistent with the latter proposal, there were no clashes when FapyGua was modeled in the *syn* conformation (Fig. 3C). The ring-opened portion of the base approximately overlays on the ThyGly ring in this structure, , and the hydrogen-bonding face is directed away from P2, E3, E6, and the 242 residue, the four key side chains, according to the mechanism postulated by Zhu with colleagues (30). Although FapyGua is usually depicted in the imidazole ring-opened aldehyde form with C8=O, the result of modeling suggested the possibility for a shift of the equilibrium to the C8-OH enol form. In such a case, the C8-OH group of FapyGua would be positioned just as close or closer to E6 than C2-OH of ThyGly in the reported crystal structure (Fig. 3 panels C and A, respectively). Based on this modeled structure, we hypothesize that similar to C2-OH in ThyGly, the C8-OH in FapyGua may mediate proton transfer from P2 to the carboxylate of E6.

The role of the 242 residue and the identity of the side chain that would protonate the base are less apparent from this model. The ultimate target of protonation, N9 of FapyGua, lies farther from K242 ζ in our model than N3 of ThyGly in the reported crystal structure ($\approx$5.4 Å and 3.5 Å, respectively). Additionally, it is even more distant from Y177 and R257, the alternative proton donors in the NEIL1 active site. We speculate that the R residue may have an advantage over the K residue in reaching the target site as it is longer and can stack under the base more effectively. This hypothetical model may explain a more efficient excision of FapyGua (and by analogy, FapyAde) by the edited K242R form.

4. Discussion

Murine models of deficiencies in DNA glycosylases have revealed the importance of maintaining genomic integrity and intracellular homeostasis. Knockouts of NEIL1, NTH1, and MYH/OGG1 have manifested with increased rates of various spontaneous and induced cancers (23, 45-49). In addition to elevated cancer risks, mice deficient in NEIL1 or OGG1 show a full spectrum of symptoms associated with metabolic syndrome, including obesity, insulin resistance, fatty liver, and dyslipidemia (7, 47, 50-56). OGG1 knockout mice are also highly resistant to pulmonary inflammation in response to allergens such as ragweed pollen extracts (57-60). These data highlight the need to understand the regulation and substrate specificities of these enzymes.

Regulation and activation of NEIL1 expression in the S-phase (9, 61), its association with the replication machinery (61-66) in its proposed "cow-catcher" role in DNA damage recognition and initiation of repair (reviewed in (67)), and pre-mRNA processing (16, 26, 27, 29, 31) likely alter the efficiency and specificity of repair processes. The additional important factors that modulate glycosylase activity of NEIL1 include its interactions with non-canonical BER components, such as high-mobility group box 1 protein (68, 69) and heterogeneous nuclear ribonucleoprotein U (70), and posttranslational modifications. Regarding the latter factor, it has been documented that acetylation of NEIL1 at Lys residues 296-298 stabilizes the formation of chromatin-bound repair complexes and increases enzymatic turnover (71). Developing a comprehensive understanding of these processes throughout development and aging are also anticipated to have considerable significance

since environmental toxicant exposures occur throughout life. Germane to this point, the Essigmann laboratory demonstrated a >10-fold increase in aflatoxin-induced mutagenesis when exposures occurred *in utero* (72).

Thus, we carried out this investigation of the unedited (K242) and edited (K242R) forms of human NEIL1. In addition to our data confirming results from prior studies demonstrating that K242 is much more active on ThyGly-containing DNA substrates, our investigation is the first to compare activities of the unedited and edited NEIL1 against two of the major, biologically relevant ring-fragmented purines, FapyAde and FapyGua. There was a modest, but statistically significant increase in catalytic efficiency in K242R for FapyAde and FapyGua. In contrast, K242R showed a lower activity on an oligodeoxynucleotide containing the AFB_1-FapyGua adduct.

Our data also demonstrate that increased catalytic efficiency for the excision of ThyGly by K242 does not expand its substrate specificity to a variety of saturated pyrimidines. Previous analyses of the bases released from γ-irradiated genomic DNAs by human and mouse NEIL1 showed that damaged pyrimidine base recognition and release was limited to ThyGly (9, 11). Mouse NEIL1 also exhibited some minor activity for 5-OH-5-MeHyd (11). In contrast, experimental designs using oligodeoxynucleotides containing site-specific 5,6-diOH-Ura, 5-OH-Ura, or 5-OH-Cyt have revealed that these damaged bases can be substrates for NEIL1 (9, 21, 73-75). Our data confirm the ability of NEIL1 to excise 5-OH-Cyt from high-molecular genomic DNA. In contrast to more efficient excision of ThyGly by K242, the efficiency of recognition of 5-OH-Cyt was enhanced by the amino acid change from K to R.

To elucidate a structural rational for the efficient recognition by NEIL1 of various purine-derived lesions, we modeled FapyGua in the NEIL1 active site, assuming that the general structure of active site in this complex would be similar to that described for ThyGly (30). The model revealed that the lesion can be accommodated only if the base adopts the *syn* orientation around the glycosidic bond. Prior modeling of the Sp-Lys adduct in the active site of a Mimivirus ortholog of human NEIL1 (MvNei1) suggested that the base also would be in the *syn* orientation (22). Thus, the *syn* conformation could be common for the purine-derived lesions in the NEIL1 active site. This is not the case for pyrimidine-derived lesions: the base of ThyGly is *anti*-oriented in structures with human NEIL1 (30) or MvNei1 (76); the 5-OH-Ura lesion can adopt both *anti* and *syn* conformation in the MvNei1 active site (76). Interestingly, in the active site of the related bacterial enzyme, formamidopyrimidine glycosylase, the carbocyclic analog of FapyGua displays the *anti* conformation, whereas 8-OH-Gua is in the *syn* conformation (77, 78).

Our modeling suggests that a shift from the free C8=O aldehyde form to the C8-OH enol form of FapyGua could direct the catalytic process towards a tautomerization-based mechanism, previously postulated for ThyGly (30). The positions of the N7 and O8 atoms in the modeled structure of the Sp-Lys adduct with MvNei1 overlap with N3 and O2 atoms in ThyGly (22), suggesting a similar mechanism. However, the data within the present study, in conjunction with prior findings (16, 26, 30), illustrated the remarkably high differential recognition of ThyGly by the two forms of NEIL1, with K242 being more efficient. The

Author Manuscript

differences were less significant or not observed for the other lesions tested and in fact, preferred NEIL1 substrates, such as FapyAde, FapyGua, Gh, and Sp, are all recognized more efficiently by the edited K242R form. Furthermore, a tautomerization-based step in NEIL1-catalyzed excision cannot be universally applied to all purine-derived substrates and in particular to various FapyGua lesions that are alkylated at the N7 site.

In conclusion, this study demonstrated differential recognition by the unedited and edited NEIL1 of several biologically significant DNA substrates, including common oxidatively-induced base lesions and the highly mutagenic AFB_1-FapyGua. The degree of modulation of NEIL1 activity by the K to R amino acid change varied. ThyGly was the only lesion recognized by two forms of NEIL1 with a great differential. In the presence of preferred NEIL1 substrates, FapyGua and FapyAde, the edited K242R form showed a very limited ability for ThyGly removal. These observations are important for understanding the mechanisms of DNA damage-induced carcinogenesis and in particular, under conditions of aberrant ADAR1-mediated editing.

Acknowledgments

Abbreviations:

8-OH-Gua	8-hydroxyguanine
ThyGly	thymine glycol
Gh	guanidinohydantoin
Sp	spiroiminohydantoin
FapyAde	4,6-diamino-5-formamidopyrimidine
FapyGua	2,6-diamino-4-hydroxy-5-formamidopyrimidine
AFB_1	aflatoxin B_1
AFB_1-FapyGua	8,9-dihydro-8-(2,6-diamino-4-oxo-3,4-dihydropyrimid-5-yl-formamido)-9-hydroxyaflatoxin B_1
HCC	hepatocellular carcinoma
8-OH-Ade	8-hydroxy-adenine
5-OH-Cyt	5-hydroxy-cytosine

5-OH-Ura	5-hydroxy-uracil
5-OH-MeHyd	5-hydroxy-5-methylhydantoin
5,6-diOH-Ura	5,6-dihydroxy-uracil
GS-MS/MS	gas chromatography-tandem mass spectrometry

References

(1). Dizdaroglu M, Coskun E and Jaruga P (2017) Repair of oxidatively induced DNA damage by DNA glycosylases: Mechanisms of action, substrate specificities and excision kinetics. Mutat Res/Mutat Res Reviews 771, 99–127.

(2). Mullins EA, Rodriguez AA, Bradley NP and Eichman BF (2019) Emerging roles of DNA glycosylases and the base excision repair pathway. Trends Biochem Sci.

(3). Fleming AM and Burrows CJ (2017) Formation and processing of DNA damage substrates for the hNEIL enzymes. Free Radic Biol Med 107, 35–52. [PubMed: 27880870]

(4). Limpose KL, Corbett AH and Doetsch PW (2017) BERing the burden of damage: Pathway crosstalk and posttranslational modification of base excision repair proteins regulate DNA damage management. DNA Repair (Amst) 56, 51–64. [PubMed: 28629773]

(5). Beard WA, Horton JK, Prasad R and Wilson SH (2019) Eukaryotic base excision repair: new approaches shine light on mechanism. Annu Rev Biochem 88, 137–162. [PubMed: 31220977]

(6). Mao P and Wyrick JJ (2019) Organization of DNA damage, excision repair, and mutagenesis in chromatin: A genomic perspective. DNA Repair (Amst), 102645.

(7). Sampath H and Lloyd RS (2019) Roles of OGG1 in transcriptional regulation and maintenance of metabolic homeostasis. DNA Repair (Amst), 102667.

(8). Bandaru V, Sunkara S, Wallace SS and Bond JP (2002) A novel human DNA glycosylase that removes oxidative DNA damage and is homologous to Escherichia coli endonuclease VIII. DNA Repair (Amst) 1, 517–529. [PubMed: 12509226]

(9). Hazra TK, Izumi T, Boldogh I, Imhoff B, Kow YW, Jaruga P, Dizdaroglu M and Mitra S (2002) Identification and characterization of a human DNA glycosylase for repair of modified bases in oxidatively damaged DNA. Proc Natl Acad Sci U S A 99, 3523–3528. [PubMed: 11904416]

(10). Morland I, Rolseth V, Luna L, Rognes T, Bjoras M and Seeberg E (2002) Human DNA glycosylases of the bacterial Fpg/MutM superfamily: an alternative pathway for the repair of 8-oxoguanine and other oxidation products in DNA. Nucleic Acids Res 30, 4926–4936. [PubMed: 12433996]

(11). Jaruga P, Birincioglu M, Rosenquist TA and Dizdaroglu M (2004) Mouse NEIL1 protein is specific for excision of 2,6-diamino-4-hydroxy-5-formamidopyrimidine and 4,6-diamino-5-formamidopyrimidine from oxidatively damaged DNA. Biochemistry 43, 15909–15914. [PubMed: 15595846]

(12). Grin IR, Rieger RA and Zharkov DO (2010) Inactivation of NEIL2 DNA glycosylase by pyridoxal phosphate reveals a loop important for substrate binding. Biochem Biophys Res Commun 394, 100–105. [PubMed: 20175991]

(13). Hailer MK, Slade PG, Martin BD, Rosenquist TA and Sugden KD (2005) Recognition of the oxidized lesions spiroiminodihydantoin and guanidinohydantoin in DNA by the mammalian base excision repair glycosylases NEIL1 and NEIL2. DNA Repair (Amst) 4, 41–50. [PubMed: 15533836]

(14). Krishnamurthy N, Zhao X, Burrows CJ and David SS (2008) Superior removal of hydantoin lesions relative to other oxidized bases by the human DNA glycosylase hNEIL1. Biochemistry 47, 7137–7146. [PubMed: 18543945]

(15). Zhao X, Krishnamurthy N, Burrows CJ and David SS (2010) Mutation versus repair: NEIL1 removal of hydantoin lesions in single-stranded, bulge, bubble, and duplex DNA contexts. Biochemistry 49, 1658–1666. [PubMed: 20099873]

(16). Prakash A, Carroll BL, Sweasy JB, Wallace SS and Doublie S (2014) Genome and cancer single nucleotide polymorphisms of the human NEIL1 DNA glycosylase: activity, structure, and the effect of editing. DNA Repair (Amst) 14, 17–26. [PubMed: 24382305]

(17). Alshykhly OR, Fleming AM and Burrows CJ (2015) 5-Carboxamido-5-formamido- 2-iminohydantoin, in addition to 8-oxo-7,8-dihydroguanine, is the major product of the iron-fenton or X-ray radiation-induced oxidation of guanine under aerobic reducing conditions in nucleoside and DNA contexts. J Org Chem 80, 6996–7007. [PubMed: 26092110]

(18). Shafirovich V, Kropachev K, Anderson T, Liu Z, Kolbanovskiy M, Martin BD, Sugden K, Shim Y, Chen X, Min JH and Geacintov NE (2016) Base and nucleotide excision repair of oxidatively generated guanine lesions in DNA. J Biol Chem 291, 5309–5319. [PubMed: 26733197]

(19). Couve S, Mace-Aime G, Rosselli F and Saparbaev MK (2009) The human oxidative DNA glycosylase NEIL1 excises psoralen-induced interstrand DNA cross-links in a three-stranded DNA structure. J Biol Chem 284, 11963–11970. [PubMed: 19258314]

(20). Martin PR, Couve S, Zutterling C, Albelazi MS, Groisman R, Matkarimov BT, Parsons JL, Elder RH and Saparbaev MK (2017) The human DNA glycosylases NEIL1 and NEIL3 excise psoralen-induced DNA-DNA cross-links in a four-stranded DNA structure. Sci Rep 7, 17438. [PubMed: 29234069]

(21). Slyvka A, Mierzejewska K and Bochtler M (2017) Nei-like 1 (NEIL1) excises 5-carboxylcytosine directly and stimulates TDG-mediated 5-formyl and 5-carboxylcytosine excision. Sci Rep 7, 9001. [PubMed: 28827588]

(22). McKibbin PL, Fleming AM, Towheed MA, Van Houten B, Burrows CJ and David SS (2013) Repair of hydantoin lesions and their amine adducts in DNA by base and nucleotide excision repair. J Am Chem Soc 135, 13851–13861. [PubMed: 23930966]

(23). Vartanian V, Minko IG, Chawanthayatham S, Egner PA, Lin YC, Earley LF, Makar R, Eng JR, Camp MT, Li L, Stone MP, Lasarev MR, Groopman JD, Croy RG, Essigmann JM, McCullough AK and Lloyd RS (2017) NEIL1 protects against aflatoxin-induced hepatocellular carcinoma in mice. Proc Natl Acad Sci U S A 114, 4207–4212. [PubMed: 28373545]

(24). Minko IG, Vartanian VL, Tozaki NN, Linde OK, Jaruga P, Coskun SH, Coskun E, Qu C, He H, Xu C, Chen T, Song Q, Jiao Y, Stone MP, Egli M, Dizdaroglu M, McCullough AK and Lloyd RS (2019) Characterization of rare NEIL1 variants found in East Asian populations. DNA Repair (Amst) 79, 32–39. [PubMed: 31100703]

(25). Minko IG, Christov PP, Li L, Stone MP, McCullough AK and Lloyd RS (2019) Processing of N^5-substituted formamidopyrimidine DNA adducts by DNA glycosylases NEIL1 and NEIL3. DNA Repair (Amst) 73, 49–54. [PubMed: 30448017]

(26). Yeo J, Goodman RA, Schirle NT, David SS and Beal PA (2010) RNA editing changes the lesion specificity for the DNA repair enzyme NEIL1. Proc Natl Acad Sci U S A 107, 20715–20719. [PubMed: 21068368]

(27). Daniel C, Silberberg G, Behm M and Ohman M (2014) Alu elements shape the primate transcriptome by cis-regulation of RNA editing. Genome Biol 15, R28. [PubMed: 24485196]

(28). Maydanovych O and Beal PA (2006) Breaking the central dogma by RNA editing. Chem Rev 106, 3397–3411. [PubMed: 16895334]

(29). Teoh PJ, An O, Chung TH, Chooi JY, Toh SHM, Fan S, Wang W, Koh BTH, Fullwood MJ, Ooi MG, de Mel S, Soekojo CY, Chen L, Ng SB, Yang H and Chng WJ (2018) Aberrant hyperediting of the myeloma transcriptome by ADAR1 confers oncogenicity and is a marker of poor prognosis. Blood 132, 1304–1317. [PubMed: 30061158]

(30). Zhu C, Lu L, Zhang J, Yue Z, Song J, Zong S, Liu M, Stovicek O, Gao YQ and Yi C (2016) Tautomerization-dependent recognition and excision of oxidation damage in base-excision DNA repair. Proc Natl Acad Sci U S A 113, 7792–7797. [PubMed: 27354518]

(31). Onizuka K, Yeo J, David SS and Beal PA (2012) NEIL1 binding to DNA containing 2'-fluorothymidine glycol stereoisomers and the effect of editing. Chembiochem 13, 1338–1348. [PubMed: 22639086]

(32). Roy LM, Jaruga P, Wood TG, McCullough AK, Dizdaroglu M and Lloyd RS (2007) Human polymorphic variants of the NEIL1 DNA glycosylase. J Biol Chem 282, 15790–15798. [PubMed: 17389588]

(33). Jaruga P, Coskun E, Kimbrough K, Jacob A, Johnson WE and Dizdaroglu M (2017) Biomarkers of oxidatively induced DNA damage in dreissenid mussels: A genotoxicity assessment tool for the Laurentian Great Lakes. Environ Toxicol 32, 2144–2153. [PubMed: 28568507]

(34). Banerjee S, Brown KL, Egli M and Stone MP (2011) Bypass of aflatoxin B_1 adducts by the Sulfolobus solfataricus DNA polymerase IV. J Am Chem Soc 133, 12556–12568. [PubMed: 21790157]

(35). Petterson EF, Goddard TD, Huang CC, Couch GS, Greenblatt DM, Meng EC and Ferrin TE (2004) UCSF Chimera – a visualization system for exploratory research and analysis. J Comput Chem 25 1605–1612. [PubMed: 15264254]

(36). Burgdorf LT and Carell T (2002) Synthesis, stability, and conformation of the formamidopyrimidine G DNA lesion. Chemistry 8, 293–301. [PubMed: 11822460]

(37). Jena NR and Mishra PC (2013) Is FapyG mutagenic?: Evidence from the DFT study. Chemphyschem 14, 3263–3270. [PubMed: 23934915]

(38). Case DA, Babin V, Berryman JT, Betz RM, Cai Q, Cerutti DS, Cheatham I, T. E., Darden TA, Duke RE, Gohlke H, Goetz AW, Gusarov S, Homeyer N, Janowski P, Kaus J, Kolossváry I, Kovalenko A, Lee TS, LeGrand S, Luchko T, Luo R, Madej B, Merz KM, Paesani F, Roe DR, Roitberg A, Sagui C, Salomon-Ferrer R, Seabra G, Simmerling CL, Smith W, Swails J, Walk-er RC, Wang J, Wolf RM, Wu X and Kollman PA (2014) AMBER14, University of California, San Francisco.

(39). Croy RG and Wogan GN (1981) Temporal patterns of covalent DNA adducts in rat liver after single and multiple doses of aflatoxin B_1. Cancer Res 41, 197–203. [PubMed: 7448760]

(40). Coskun E, Jaruga P, Vartanian V, Erdem O, Egner PA, Groopman JD, Lloyd RS and Dizdaroglu M (2019) Aflatoxin-guanine DNA adducts and oxidatively-induced DNA damage in aflatoxin-treated mice in vivo as measured by liquid chromatographytandem mass spectrometry with isotope-dilution. Chem Res Toxicol 32, 80–89. [PubMed: 30525498]

(41). Lin YC, Li L, Makarova AV, Burgers PM, Stone MP and Lloyd RS (2014) Molecular basis of aflatoxin-induced mutagenesis-role of the aflatoxin B_1-formamidopyrimidine adduct. Carcinogenesis 35, 1461–1468. [PubMed: 24398669]

(42). Chawanthayatham S, Valentine CC 3rd, Fedeles BI, Fox EJ, Loeb LA, Levine SS, Slocum SL, Wogan GN, Croy RG and Essigmann JM (2017) Mutational spectra of aflatoxin B_1 in vivo establish biomarkers of exposure for human hepatocellular carcinoma. Proc Natl Acad Sci U S A 114, E3101–E3109. [PubMed: 28351974]

(43). Huang MN, Yu W, Teoh WW, Ardin M, Jusakul A, Ng AWT, Boot A, Abedi-Ardekani B, Villar S, Myint SS, Othman R, Poon SL, Heguy A, Olivier M, Hollstein M, Tan P, Teh BT, Sabapathy K, Zavadil J and Rozen SG (2017) Genome-scale mutational signatures of aflatoxin in cells, mice, and human tumors. Genome Res 27, 1475–1486. [PubMed: 28739859]

(44). Zhang W, He H, Zang M, Wu Q, Zhao H, Lu LL, Ma P, Zheng H, Wang N, Zhang Y, He S, Chen X, Wu Z, Wang X, Cai J, Liu Z, Sun Z, Zeng YX, Qu C and Jiao Y (2017) Genetic features of aflatoxin-associated hepatocellular carcinoma. Gastroenterology 153, 249–262 e242. [PubMed: 28363643]

(45). Xie Y, Yang H, Cunanan C, Okamoto K, Shibata D, Pan J, Barnes DE, Lindahl T, McIlhatton M, Fishel R and Miller JH (2004) Deficiencies in mouse Myh and Ogg1 result in tumor predisposition and G to T mutations in codon 12 of the K-ras oncogene in lung tumors. Cancer Res 64, 3096–3102. [PubMed: 15126346]

(46). Russo MT, De Luca G, Degan P, Parlanti E, Dogliotti E, Barnes DE, Lindahl T, Yang H, Miller JH and Bignami M (2004) Accumulation of the oxidative base lesion 8-hydroxyguanine in DNA of tumor-prone mice defective in both the Myh and Ogg1 DNA glycosylases. Cancer Res 64, 4411–4414. [PubMed: 15231648]

(47). Vartanian V, Lowell B, Minko IG, Wood TG, Ceci JD, George S, Ballinger SW, Corless CL, McCullough AK and Lloyd RS (2006) The metabolic syndrome resulting from a knockout of the NEIL1 DNA glycosylase. Proc Natl Acad Sci U S A 103, 1864–1869. [PubMed: 16446448]

(48). Chan MK, Ocampo-Hafalla MT, Vartanian V, Jaruga P, Kirkali G, Koenig KL, Brown S, Lloyd RS, Dizdaroglu M and Teebor GW (2009) Targeted deletion of the genes encoding NTH1 and NEIL1 DNA N-glycosylases reveals the existence of novel carcinogenic oxidative damage to DNA. DNA Repair (Amst) 8, 786–794. [PubMed: 19346169]

(49). Yamamoto ML, Chapman AM and Schiestl RH (2013) Effects of side-stream tobacco smoke and smoke extract on glutathione- and oxidative DNA damage repair-deficient mice and blood cells. Mutat Res 749, 58–65. [PubMed: 23748015]

(50). Sampath H, Batra AK, Vartanian V, Carmical JR, Prusak D, King IB, Lowell B, Earley LF, Wood TG, Marks DL, McCullough AK and L RS (2011) Variable penetrance of metabolic phenotypes and development of high-fat diet-induced adiposity in NEIL1-deficient mice. Am J Physiol Endocrinol Metab 300, E724–734. [PubMed: 21285402]

(51). Sampath H, Vartanian V, Rollins MR, Sakumi K, Nakabeppu Y and Lloyd RS (2012) 8-Oxoguanine DNA glycosylase (OGG1) deficiency increases susceptibility to obesity and metabolic dysfunction. PLoS One 7, e51697. [PubMed: 23284747]

(52). Sampath H, McCullough AK and Lloyd RS (2012) Regulation of DNA glycosylases and their role in limiting disease. Free Radic Res 46, 460–478. [PubMed: 22300253]

(53). Sampath H (2014) Oxidative DNA damage in disease–insights gained from base excision repair glycosylase-deficient mouse models. Environ Mol Mutagen 55, 689–703. [PubMed: 25044514]

(54). Vartanian V, Tumova J, Dobrzyn P, Dobrzyn A, Nakabeppu Y, Lloyd RS and Sampath H (2017) 8-oxoguanine DNA glycosylase (OGG1) deficiency elicits coordinated changes in lipid and mitochondrial metabolism in muscle. PLoS One 12, e0181687. [PubMed: 28727777]

(55). Komakula SSB, Tumova J, Kumaraswamy D, Burchat N, Vartanian V, Ye H, Dobrzyn A, Lloyd RS and Sampath H (2018) The DNA repair protein OGG1 protects against obesity by altering mitochondrial energetics in white adipose tissue. Sci Rep 8, 14886. [PubMed: 30291284]

(56). Sharma P and Sampath H (2019) Mitochondrial DNA Integrity: Role in health and disease. Cells 8.

(57). Bacsi A, Aguilera-Aguirre L, Szczesny B, Radak Z, Hazra TK, Sur S, Ba X and Boldogh I (2013) Down-regulation of 8-oxoguanine DNA glycosylase 1 expression in the airway epithelium ameliorates allergic lung inflammation. DNA Repair (Amst) 12, 18–26. [PubMed: 23127499]

(58). Aguilera-Aguirre L, Bacsi A, Radak Z, Hazra TK, Mitra S, Sur S, Brasier AR, Ba X and Boldogh I (2014) Innate inflammation induced by the 8-oxoguanine DNA glycosylase-1-KRAS-NF-kB pathway. J Immunol 193, 4643–4653. [PubMed: 25267977]

(59). Aguilera-Aguirre L, Hao W, Pan L, Li X, Saavedra-Molina A, Bacsi A, Radak Z, Sur S, Brasier AR, Ba X and Boldogh I (2017) Pollen-induced oxidative DNA damage response regulates miRNAs controlling allergic inflammation. Am J Physiol Lung Cell Mol Physiol 313, L1058–L1068. [PubMed: 28798252]

(60). Visnes T, Cazares-Korner A, Hao W, Wallner O, Masuyer G, Loseva O, Mortusewicz O, Wiita E, Sarno A, Manoilov A, Astorga-Wells J, Jemth AS, Pan L, Sanjiv K, Karsten S, Gokturk C, Grube M, Homan EJ, Hanna BMF, Paulin CBJ, Pham T, Rasti A, Berglund UW, von Nicolai C, Benitez-Buelga C, Koolmeister T, Ivanic D, Iliev P, Scobie M, Krokan HE, Baranczewski P, Artursson P, Altun M, Jensen AJ, Kalderen C, Ba X, Zubarev RA, Stenmark P, Boldogh I and Helleday T (2018) Small-molecule inhibitor of OGG1 suppresses proinflammatory gene expression and inflammation. Science 362, 834–839. [PubMed: 30442810]

(61). Hegde ML, Hegde PM, Bellot LJ, Mandal SM, Hazra TK, Li GM, Boldogh I, Tomkinson AE and Mitra S (2013) Prereplicative repair of oxidized bases in the human genome is mediated by NEIL1 DNA glycosylase together with replication proteins. Proc Natl Acad Sci U S A 110, E3090–3099. [PubMed: 23898192]

(62). Das A, Boldogh I, Lee JW, Harrigan JA, Hegde ML, Piotrowski J, de Souza Pinto N, Ramos W, Greenberg MM, Hazra TK, Mitra S and Bohr VA (2007) The human Werner syndrome protein stimulates repair of oxidative DNA base damage by the DNA glycosylase NEIL1. J Biol Chem 282, 26591–26602. [PubMed: 17611195]

(63). Guan X, Bai H, Shi G, Theriot CA, Hazra TK, Mitra S and Lu AL (2007) The human checkpoint sensor Rad9-Rad1-Hus1 interacts with and stimulates NEIL1 glycosylase. Nucleic Acids Res 35, 2463–2472. [PubMed: 17395641]

(64). Theriot CA, Hegde ML, Hazra TK and Mitra S (2010) RPA physically interacts with the human DNA glycosylase NEIL1 to regulate excision of oxidative DNA base damage in primer-template structures. DNA Repair (Amst) 9, 643–652. [PubMed: 20338831]

(65). Hegde PM, Dutta A, Sengupta S, Mitra J, Adhikari S, Tomkinson AE, Li GM, Boldogh I, Hazra TK, Mitra S and Hegde ML (2015) The C-terminal domain (CTD) of human DNA glycosylase NEIL1 is required for forming BERosome repair complex with DNA replication proteins at the replicating genome: dominant negative function of the CTD. J Biol Chem 290, 20919–20933. [PubMed: 26134572]

(66). Prakash A, Moharana K, Wallace SS and Doublie S (2017) Destabilization of the PCNA trimer mediated by its interaction with the NEIL1 DNA glycosylase. Nucleic Acids Res 45, 2897–2909. [PubMed: 27994037]

(67). Rangaswamy S, Pandey A, Mitra S and Hegde ML (2017) Pre-replicative repair of oxidized bases maintains fidelity in mammalian genomes: the cowcatcher role of NEIL1 DNA glycosylase. Genes (Basel) 8.

(68). Liu Y, Prasad R and Wilson SH (2010) HMGB1: roles in base excision repair and related function. Biochim Biophys Acta 1799, 119–130. [PubMed: 20123074]

(69). Prasad R, Liu Y, Deterding LJ, Poltoratsky VP, Kedar PS, Horton JK, Kanno S, Asagoshi K, Hou EW, Khodyreva SN, Lavrik OI, Tomer KB, Yasui A and Wilson SH (2007) HMGB1 is a cofactor in mammalian base excision repair. Mol Cell 27, 829–841. [PubMed: 17803946]

(70). Hegde ML, Banerjee S, Hegde PM, Bellot LJ, Hazra TK, Boldogh I and Mitra S (2012) Enhancement of NEIL1 protein-initiated oxidized DNA base excision repair by heterogeneous nuclear ribonucleoprotein U (hnRNP-U) via direct interaction. J Biol Chem 287, 34202–34211. [PubMed: 22902625]

(71). Sengupta S, Yang C, Hegde ML, Hegde PM, Mitra J, Pandey A, Dutta A, Datarwala AT, Bhakat KK and Mitra S (2018) Acetylation of oxidized base repair-initiating NEIL1 DNA glycosylase required for chromatin-bound repair complex formation in the human genome increases cellular resistance to oxidative stress. DNA Repair (Amst) 66-67, 1–10. [PubMed: 29698889]

(72). Chawanthayatham S, Thiantanawat A, Egner PA, Groopman JD, Wogan GN, Croy RG and Essigmann JM (2015) Prenatal exposure of mice to the human liver carcinogen aflatoxin B_1 reveals a critical window of susceptibility to genetic change. Int J Cancer 136, 1254–1262. [PubMed: 25070670]

(73). Hazra TK and Mitra S (2006) Purification and characterization of NEIL1 and NEIL2, members of a distinct family of mammalian DNA glycosylases for repair of oxidized bases. Methods Enzymol 408, 33–48. [PubMed: 16793361]

(74). Hegde ML, Hegde PM, Arijit D, Boldogh I and Mitra S (2012) Human DNA glycosylase NEIL1's interactions with downstream repair proteins is critical for efficient repair of oxidized DNA base damage and enhanced cell survival. Biomolecules 2, 564–578. [PubMed: 23926464]

(75). Kladova OA, Grin IR, Fedorova OS, Kuznetsov NA and Zharkov DO (2019) Conformational dynamics of damage processing by human DNA glycosylase NEIL1. J Mol Biol 6, 1098–1112.

(76). Imamura K, Averill A, Wallace SS and Doublie S (2012) Structural characterization of viral ortholog of human DNA glycosylase NEIL1 bound to thymine glycol or 5-hydroxyuracil-containing DNA. J Biol Chem 287, 4288–4298. [PubMed: 22170059]

(77). Fromme JC and Verdine GL (2003) DNA lesion recognition by the bacterial repair enzyme MutM. J Biol Chem 278, 51543–51548. [PubMed: 14525999]

(78). Coste F, Ober M, Carell T, Boiteux S, Zelwer C and Castaing B (2004) Structural basis for the recognition of the FapydG lesion (2,6-diamino-4-hydroxy-5-formamidopyrimidine) by formamidopyrimidine-DNA glycosylase. J Biol Chem 279, 44074–44083. [PubMed: 15249553]
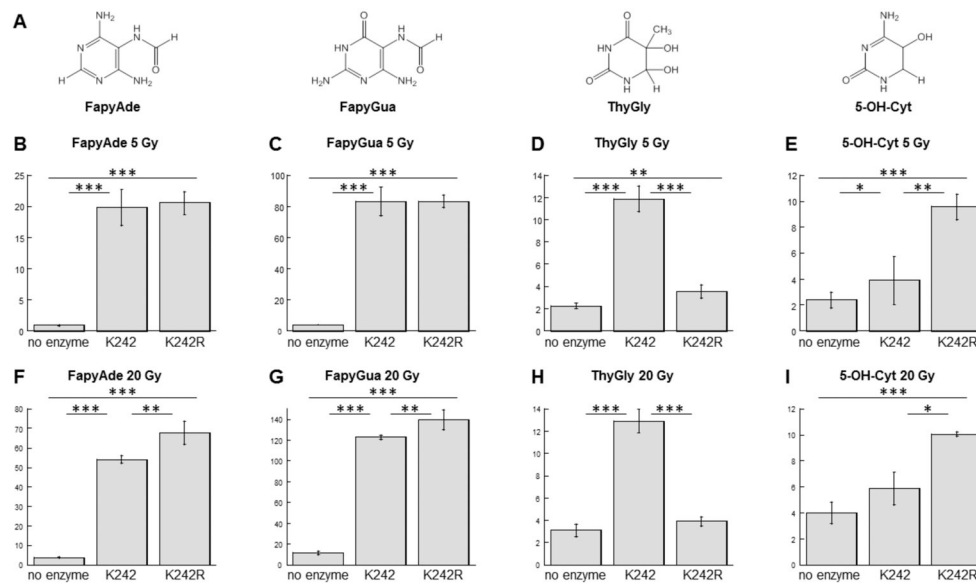
Figure 1.
NEIL1-catalyzed removal of oxidatively-induced DNA base lesions (A) from high-molecular weight genomic DNA. The calf thymus DNA exposed to 5 Gy (B-E) or 20 Gy (F-I) γ-irradiation dose was incubated with no enzyme or in the presence of the unedited or edited NEIL1. The released FapyAde (B & F), FapyGua (C & G), ThyGly (D & H), and 5-OH-Cyt (E & I) were measured by GC-MS/MS using their stable isotope-labeled analogues as internal standards. * = $p < 0.05$; ** = $p < 0.01$; *** = $p < 0.001$. The uncertainties are standard deviations.
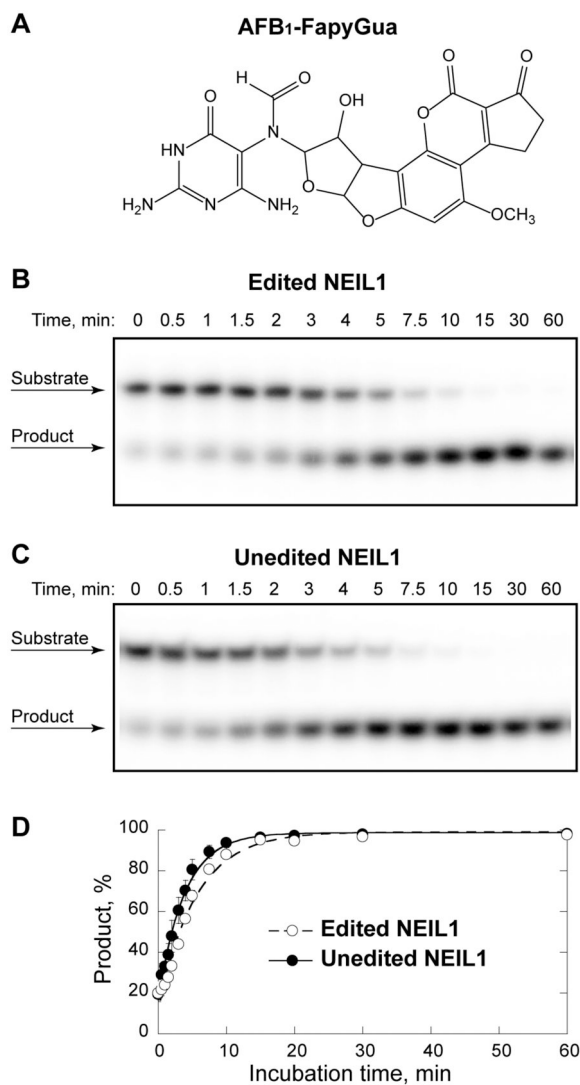
Figure 2.
NEIL1-catalyzed excision of AFB$_1$-FapyGua. The reactions were conducted using 24-mer double-stranded DNA substrate that contained a centrally-located AFB$_1$-FapyGua (**A**). Representative gel images for the edited (**B**) and unedited (**C**) NEIL1 are shown. The data shown in plot (**D**) demonstrate the time-dependent product accumulation, with fit of these data that were obtained from three independent experiments (average ± standard deviation) to a single exponential equation (correlation coefficient R > 0.99 for each enzyme).
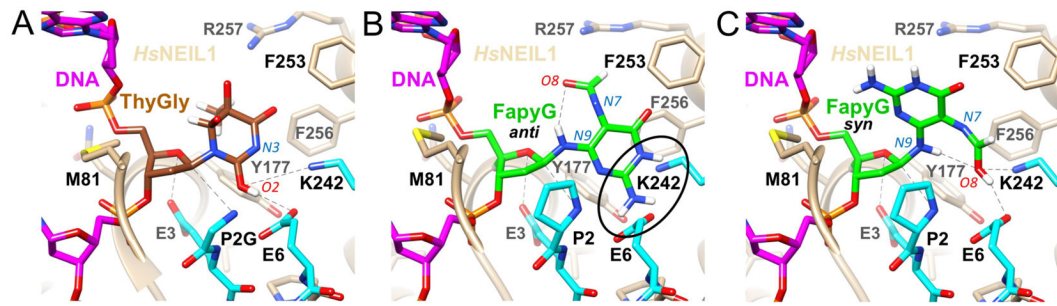
Figure 3.
Modeling the FapyGua structure in the NEIL1 active site. Structure of ThyGly in the K242 NEIL1 active site (A). Modeled FapyGua in the K242 NEIL1 active site with base in the *anti* (B) or *syn* (C) configuration. Selected residues and atoms are labeled and key interactions are indicated with dashed lines.